

GamesBond: Bimanual Haptic Illusion of Physically Connected Objects for Immersive VR Using Grip Deformation

Neung Ryu
Industrial Design, KAIST
Daejeon, Republic of Korea
n.ryu@kaist.ac.kr

Hye-Young Jo
Industrial Design, KAIST
Daejeon, Republic of Korea
hyeyoungjo@kaist.ac.kr

Michel Pahud
Microsoft Research
Redmond, WA, USA
mpahud@microsoft.com

Mike Sinclair
Microsoft Research
Redmond, WA, USA
sinclair@microsoft.com

Andrea Bianchi
Industrial Design, KAIST
Daejeon, Republic of Korea
andrea@kaist.ac.kr

ABSTRACT

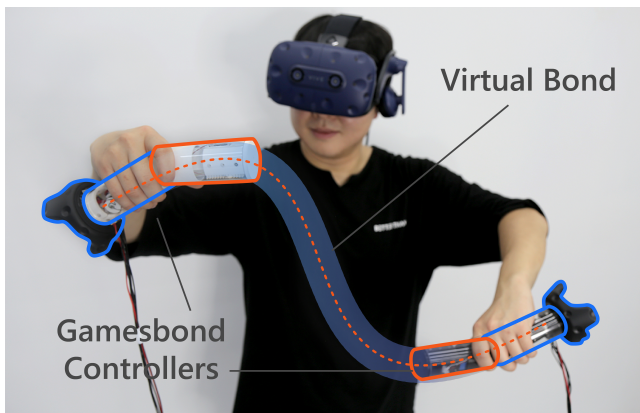


Figure 1: GamesBond creates the illusion of a physical connection (e.g. a rope) by rendering the grip deformations in a pair of separate controllers. The blue shade indicates the virtual bond as perceived by the user, while the dotted orange line shows the centerline that the GamesBond controllers approximate to render the object.

Virtual Reality experiences, such as games and simulations, typically support the usage of bimanual controllers to interact with virtual objects. To recreate the haptic sensation of holding objects of various shapes and behaviors with both hands, previous researchers have used mechanical linkages between the controllers that render adjustable stiffness. However, the linkage cannot quickly adapt to simulate dynamic objects, nor it can be removed to support free movements. This paper introduces GamesBond, a pair of 4-DoF controllers without physical linkage but capable to create the illusion

Permission to make digital or hard copies of all or part of this work for personal or classroom use is granted without fee provided that copies are not made or distributed for profit or commercial advantage and that copies bear this notice and the full citation on the first page. Copyrights for components of this work owned by others than ACM must be honored. Abstracting with credit is permitted. To copy otherwise, or republish, to post on servers or to redistribute to lists, requires prior specific permission and/or a fee. Request permissions from permissions@acm.org.

CHI '21, May 8–13, 2021, Yokohama, Japan

© 2021 Association for Computing Machinery.

ACM ISBN 978-1-4503-8096-6/21/05...\$15.00

<https://doi.org/10.1145/3411764.3445727>

of being connected as a single device, forming a virtual *bond*. The two controllers work together by dynamically displaying and physically rendering deformations of hand grips, and so allowing users to perceive a single connected object between the hands, such as a jumping rope. With a user study and various applications we show that GamesBond increases the realism, immersion, and enjoyment of bimanual interaction.

CCS CONCEPTS

• **Human-centered computing** → **Human computer interaction (HCI)**.

KEYWORDS

Haptics, bimanual interaction, grip deformation, shape-changing, Virtual Reality

ACM Reference Format:

Neung Ryu, Hye-Young Jo, Michel Pahud, Mike Sinclair, and Andrea Bianchi. 2021. GamesBond: Bimanual Haptic Illusion of Physically Connected Objects for Immersive VR Using Grip Deformation. In *CHI Conference on Human Factors in Computing Systems (CHI '21)*, May 8–13, 2021, Yokohama, Japan. ACM, New York, NY, USA, 10 pages. <https://doi.org/10.1145/3411764.3445727>

1 INTRODUCTION

It is widely known that haptic controllers can enhance the realism and immersion of Virtual Reality (VR) experiences [16, 21]. While most of the haptic research focuses on enhancing a single controller [35, 39, 40], typical VR interactive applications such as games and simulators leverage bimanual input with a pair of controllers and require coordinated movements of both hands. There are numerous examples of bimanual coordinated input techniques in VR applications [14, 28, 31], but only a few examples of bimanual haptic controllers. Most of the related work describe earth-grounded (therefore fixed in space) devices [24, 27], or single controller devices that can be grasped with two hands [12, 29]. The Haptic Links [34] is a notable exception, describing a pair of independently movable off-the-shelf controllers that can be physically connected through a mechanical link to render a variety of two-handed objects. However, because a physical locking mechanism between the two controllers is required to render the stiffness felt between the hands, the ease, speed, and the degrees of differential freedom at which the user can move the controllers is limited. This limitation

makes it impossible, for example, to render the haptics of highly dynamic objects with many degrees of freedom, such as a jumping rope held in the hands.

This paper introduces GamesBond, a pair of 4-DoF controllers with no physical linkage between them but still capable of creating the haptic illusion of a virtual *bond* connecting the controllers as a single device. This illusion is grounded in Guiard’s reference principles of asymmetric division of labor for bimanual actions [7], which also applies to kinesthetic feedback [1]. These principles describe how the kinesthetic sense of one hand movements are relative to the other — known as a *kinesthetic reference frame* [1]. GamesBond exploits this experience by mechanically changing the shape of one or both controllers’ handle (via bending, twisting or stretching), and resulting in kinesthetic deformations of the skin. The user’s interpretation of these differential deformations instills the illusion of a single coordinated motion which the human brain, aided by visual feedback in a VR application, interprets as a connected object. Figure 1 shows a simplified representation of how a user experiences the deformation of a virtual soft object held in the hands when rendered by the GamesBond controllers.

The rest of the paper is structured in the following way: 1) we introduce the underlying mechanism of GamesBond, explaining the principle of how the haptic bonds are computed and rendered; 2) we present the design, implementation, and technical evaluation of the GamesBond controllers — a pair of two 4-DoF grip deformation devices capable of bending (2-DOF), twisting (1-DOF), and stretching (1-DOF); 3) through a user study with 12 participants and a series of applications we demonstrate that GamesBond realistically conveys the haptic illusion of stiff, soft, and dynamic objects held in two hands, without requiring a physical connection.

2 RELATED WORK

Our research has been inspired by previous work on bimanual haptic controllers, and shape-changing controllers that cause deformations in the user’s hands.

2.1 Bimanual haptic controllers

There are numerous examples in literature of bimanual grounded haptic devices (e.g., [3, 17, 19, 20, 24]), but in this review we mainly focus on ungrounded controllers (not fixed in space), since they are more common for commercial VR systems.

SPRING [11] is a pair of handheld controllers connected together by a spring that creates the illusion of holding and manipulating a three-dimensional object. The handles are connected by a spring, which generates differential compliant forces. Haptic Links [34] uses mechanically actuated connections between two VR controllers. The authors designed three types of mechanically actuated connections to create various constraints between hands, which are used to render objects such as a bow and arrow, a rifle, or a trombone. LevioPole [29] and Aero-Plane [16] explore alternative form factors, providing mid-air haptic feedback and full-body interaction using multiple fans attached to a controller that can be grasped with both hands. TorqueBar [36] exploits the dynamic inertia and the change of center of gravity to simulate weight movements in one dimension that can be used for games or robot navigation. Alternative approaches use grain vibrations to create the illusion

of objects deformed with both hands[12], or the out-of-body touch illusion on a virtual bar hold between two separate controllers [6]. In the case of Gonzalez et al., researchers focused on bimanual haptic retargeting in VR, and studied the tendency of detection rate according to 64 different combinations of right and left hand offsets [5].

Similarly to these approaches, GamesBond also leverage on bimanual interaction. However, it creates the illusion of a connected object between the controllers leaving the hands unconstrained.

2.2 Shape-changing haptic controllers

Researchers have been exploring controllers that deform in the user’s hand to feel shapes and also controllers that are changing shape or weight distribution to create different haptic sensations.

Krekhov et al., [18] introduces a self-transforming controller that can change its shape from a tiny blaster size to a big rifle (grasped in two hands) using a telescopic extension. PACAPA [35] and Hapmap [15] are handheld devices that render haptic feedback onto a user’s palm either when the user interacts with virtual tools, such as a stick, or for navigation purpose. POCOPO [39] proposes a similar approach, but it is based on a pin-array built into the controller’s handle. The authors show that it can create real-time illusions of objects changing shape in the hand. HaptiVec [4] is similar of POCOPO but uses a lower resolution display, mainly capable of conveying directions. PuPoP [37] took another approach, inflating and deflating a pneumatic proxy interface to provide the haptic sensation of graspable objects with predetermined shapes. Nakagaki et al. [25] explored a new technique to deliver more authentic experience to user, by suggesting a stick-shaped device that can mimic the movement of another person’s stick-shape tool through 2-DoF deformations.

Murray et al. [22] describes a controller that can modify its shape and also its stiffness by inflating and deflating a handle. The works by Guinan et al. [8, 9] use instead four one-dimensional translations in different directions to generate the illusion of torque and rotational inertia. Two-dimensional translations are used in [32, 33] to convey directions for navigation. Planar translations applied between the finger and thumb are used in [38] to create the feeling of stretching, twisting, and rotation cues. Finally, the authors of GraspForm [10] developed a haptic display that conveys via grasp the shapes, hardness, and textures of objects displayed on a 3D haptic TVs. The device can render the surface shapes and hardness of a virtual object.

Additionally, researchers have been working on VR Controllers that change weight position or air drag. Shifty [40] enhanced the user’s perception of virtual objects by automatically changing its internal weight distribution. Transcalibur [30] is a controller that physically moves a weight in 2D for rendering the illusion of holding different objects. Drag:On [41] changes the drag and rotational inertia felt by the user by dynamically adjusting its surface area, resulting in the illusion of different virtual mechanical resistance.

GamesBond takes numerous inspiration from these works. However, differently from these shape-changing controllers which were mainly designed for single-hand interactions, it is designed to work using both hands.

3 GAMESBOND SYSTEM

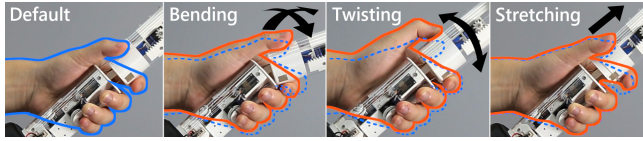


Figure 2: GamesBond’s 4-DoF deformations and corresponding hand grips. Blue and orange lines indicate the initial and deformed grips respectively.

GamesBond is a pair of controllers with handles constructed with two segments, and capable of configuring in different shapes (Figure 2). The upper segment of the controller can *bend* (in the pitch and yaw direction), *twist* (roll direction), and *stretch* (or compress) along its length, relative to the lower segment. These deformations are perceived by the user when wielding the device in the middle of the handle, with the fingers and the palm simultaneously gripping both segments (e.g., Figure 2). Using a VIVE tracker attached to the bottom of each controller, GamesBond can then track the coordinates of each controller and use them to compute how a virtual object between these two points would move or deform. The resulting geometry is used to guide the actuation of the shape-changing controllers through bending, twisting and stretching. The next sections describe the mechanical transformations and the computation of the virtual bonds. Finally, we describe in detail the hardware specifications.

3.1 Mechanism

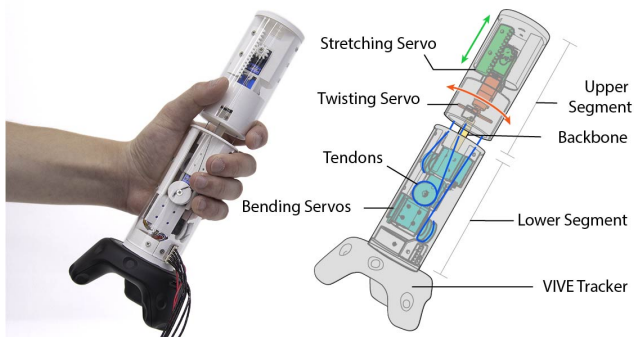


Figure 3: Details of mechanical structure of the controller.

GamesBond renders 4-DoF transformations using five servomotors. **Bending** is rendered through the antagonistic behavior of three tendons connecting the two segments of the handle. The three tendons are evenly spaced around a silicone backbone connecting the segments, with one end of each tendon firmly attached to the base of the top segment, and the other end connected to a servomotor winch in the lower segment (Figure 3). To bend the controller, the length of each tendon is adjusted such that it is proportionally shorter in the direction of bending, as shown in the formula in Figure 4. Our configuration allows the top segment to bend up to 30° in arbitrary directions, achieving 2-DoF.

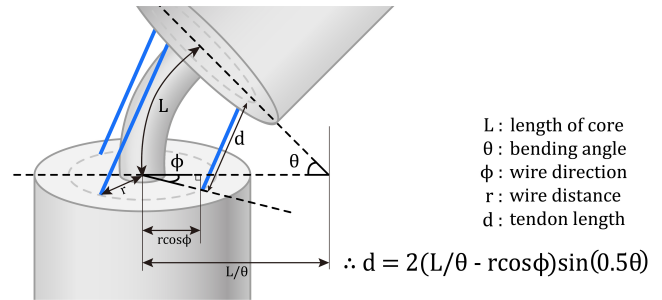


Figure 4: Tendons layout and length calculation.

Twisting and **stretching** are achieved by moving the outer shell of the upper segment (both achieving 1-DoF). Specifically, twisting works using an inner servo that rotates the outer shell between -70° and 70° . For stretching, another inner servo drives a rack and pinion mechanism that pushes or pulls the outer shell between -2.5 mm and 9 mm (0 mm being the neutral state).

3.2 Virtual Bonds

Exemplifying the rendering capability of GamesBond, we implemented three different simulations for three types of *bonds* with discretely distinct features: rigid, soft, and dynamic materials. These simulations are computed in real-time using Unity3D, running on a PC equipped with an i7-8700 CPU at 3.20 Ghz, 16 GB of RAM, and NVIDIA GeForce GTX 1060 (6 GB) graphic card. The average refresh rate of the software calculations was measured as 200Hz. The results of these computations are simultaneously presented via a graphical feedback in the VR headset, and sent over serial to the controllers for haptic rendering.

All bonds described below share similar characteristics: they represent a physical link of various material, with a length of 500 mm (l). These bodies are visually rendered as white surfaces connected to two red handles, whose position and rotation is mapped to the physical location and orientation of the controllers.



Figure 5: Visual and haptic renderings of three example bonds: (a) Rigid, (b) Soft, and (c) Dynamic.

A *rigid bond* (Figure 5.a) is a completely non-deformable connection that feels as a mechanical rigid constraint in the users’ hands. To render the position ($P(t)$) and rotation ($R(t)$) of each vertex t of the bond we used Equation (1) where l indicates the initial length of the virtual bond. Specifically, for bending the tip of the upper segment, each controller is oriented to align with the centroid of

the rigid bond — i.e., the middle point between the left (P_L) and right (P_R) hand. The upper segment of the controller also stretches or compresses trying to match the coordinates of the endpoints of the virtual rigid object (the points where $t = 0$ and $t = 1$). Analogously, the controller twists ($R(t)$) in order to align with the bond's longitudinal rotation (described as the mean rotation between the hands - R_L and R_R).

$$\begin{aligned} \mathbf{P}(t) &= \frac{\mathbf{P}_L + \mathbf{P}_R}{2} + \left(\frac{1}{2} - t\right) \left(\frac{l}{|\mathbf{P}_L - \mathbf{P}_R|}\right) (\mathbf{P}_L - \mathbf{P}_R), \\ \mathbf{R}(t) &= \frac{\mathbf{R}_L + \mathbf{R}_R}{2}, \quad (0 \leq t \leq 1) \end{aligned} \quad (1)$$

A *soft bond* (Figure 5.b) corresponds to a deformable and pliable connection without oscillations, like a gooseneck camera mount. In such case, the shape assumed by the bond can be described as a function of the controllers' position. We computed the shape of the bond as a cubic bezier curve, as described in Equation (2).

$$\begin{aligned} \mathbf{P}(t) &= (1-t)^3 \mathbf{P}_L + 3(1-t)^2 t \mathbf{P}_{LH} + 3(1-t)t^2 \mathbf{P}_{RH} + t^3 \mathbf{P}_R, \\ \mathbf{R}(t) &= (1-t) \mathbf{R}_L + t \mathbf{R}_R, \quad (0 \leq t \leq 1). \end{aligned} \quad (2)$$

In this equation, the anchor points (P_L, P_R) are the center points of the user's grip (i.e., the middle point of the flexible backbone connecting the two segments), and the handles (P_{LH}, P_{RH}) are the points placed 200 mm above the anchor points along the longitudinal axis of the lower segment. Accordingly, both the anchor point and the handle always have a fixed position relative to the lower segment. Therefore, the anchor points become the starting points of the bond, and the handles control the tangential direction of the curve. The position of all the vertices $P(t)$ of the soft bond is then computed using the parameter t , representing the relative location between two anchors. Finally, twisting $R(t)$ was calculated by linearly interpolating each of the point at t using the roll of each controller (R_L, R_R).

Finally, the *dynamic bond* (Figure 5.c) is a soft bond with varying kinematic properties, capable of rendering inertia and oscillations. It is perceived by the users as an elastic rope. To simulate the dynamics of this bond, we used the off-the-shelf Obi Rope¹ asset available from the Unity Store which utilizes the XPBD method [23] to provide a lightweight simulation. Its properties were configured in software to match a mass of 1 kg, with a Young's module of 12 kPa, roughly corresponding to the elasticity of a dough [26].

3.3 Technical Implementation

GamesBond is composed of two segments. Each segment is enclosed in a 2 mm thick acrylic shell with a diameter of 45 mm. The upper segment is 97 mm long, and the lower one is 110 mm. The two segments are separated by a 12 mm gap and held together by a 7 mm diameter silicon rubber backbone. Inside the controllers there are five servomotors (MG92B) with 3D-printed mounts fabricated using Polylactic Acid (PLA) thermoplastic. Servomotors are operated at 6 V, and are capable of 3.5 kgf-cm at 0.65 A. The tendons used for bending are made of polyethylene, having a diameter of 0.5 mm and evenly spaced 120° apart around the center, with a radial distance of 15 mm. Finally, a VIVE tracker is attached at the bottom of the

¹<http://obi.virtualmethodstudio.com>

lower segment. The total length of the device is 261 mm, and its weight is 284g.

Operating electronics and power supply are offloaded in a separated PCB, connected via long wires to the controllers. This setup allows the controllers to be lightweight. Two Arduino Mega (one for each controller) drives the servos via a PWM signal. The device power consumption is 19.5W per controller.

4 TECHNICAL EVALUATION

We conducted two complementary technical evaluations to characterize the rendering capabilities of the GamesBond controllers. In the first evaluation we measured the accuracy and the speed of the shape changing mechanism for bending, stretching and twisting. This allows us to estimate how quickly and reliably the controller can be driven to specified shapes. In the second evaluation we aim to understand the effect of the user's grip force. Therefore, we attempted to determine the force maximum threshold, and in which situation and how often any of the internal motors would reach its maximum capabilities (e.g., stalling current). For all tests we used only a single controller and was augmented with additional sensing hardware to collect electric current measurements for each individual internal servo motor.

4.1 Position Control

To accurately measure the output displacement of the device, we equipped a GamesBond controller with four lightweight reflective markers tracked using an OptiTrack system as shown in Figure 6. We then fixed the lower segment of the device on a desk using clamps. Using custom software written in Unity, we instructed the device to move to specified configurations. We then sampled the controller's coordinate information using a V120: Trio camera, positioned 80 cm in front of the controller. Sampled points were acquired using the Motive software, then exported to Unity and compared with the original input.

Input movements were specified for bending, twisting and stretching motions separately. For bending, we collected measurements of 216 points placed at intervals of 5° along the polar angle, in the range between 5°-30°, and at intervals of 10° along the azimuthal angle between 0°-350°. We also collected measures of twisting for 29 distinct points (-70° to 70°, with 5° resolution), and of stretching for 24 points (-2.5 mm to 9.0, with 0.5 mm resolution). These samples were collected 10 times, and mean results of displacement errors are shown in Figure 6. Blue circles indicate the intended positions and the red lines show the direction and amount of the error between the intended and actual output positions. To calculate the average error, we used a mean absolute error to prevent canceling errors with opposite directions. For bending, we report a mean absolute error of 0.31° (standard deviation SD: 0.26°) along the polar angle, and 1.92° (SD: 1.11°) along the azimuth angle. Mean error for twisting was 1.21° (SD: 0.55°), and for stretching was 0.08 mm (SD: 0.05 mm).

In order to evaluate GamesBond's rendering latency and maximum frequency of movement, we adapted a method described in related previous work [16]. We measured the rise time (from 0 to 90% of the desired input) for bending, twisting and stretching in their maximum operative ranges (bending: from 0 to 30°; twisting:

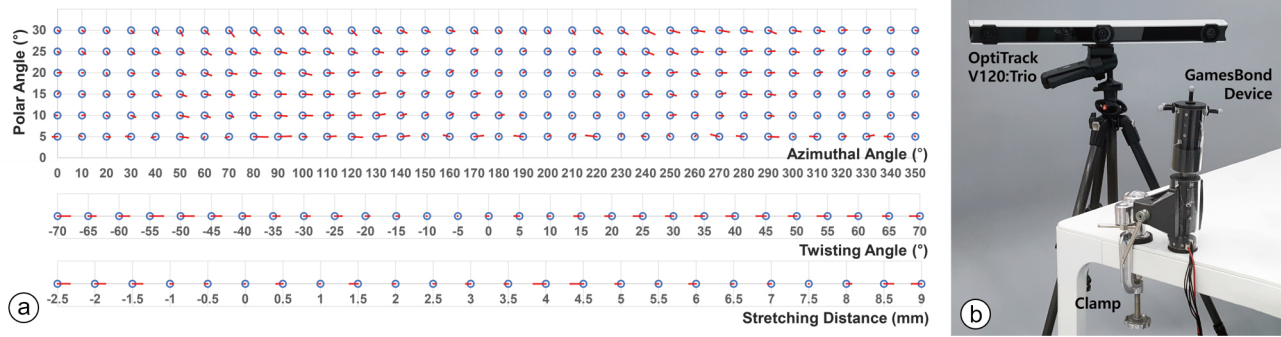


Figure 6: (a) Desired input positions (blue circles) and amount of delta error for output (red lines); (b) evaluation setup using OptiTrack system.

from -70 to 70° ; stretching: from -2.5 mm to 9 mm). In the case of bending, in order to cancel out any effect due to direction (i.e., polar angle), we performed the measurements 36 times at intervals of 10° . All measurements were repeated 10 times. As a result, the mean rise time of the bending, twisting, stretching were measured as 153.1 (SD: 7.2), 292.5 (SD: 5.0), and 274.7 (SD: 4.8) milliseconds.

4.2 Maximum Force and Torque

The following two tests describe the controller's force and torque under stress – maximum stall force and the user's typical grip force during usage.

In the first test we separately measured the stall force and torque for each of the three types of motion (bending, twisting, stretching) using a push-pull gauge. A controller was firmly attached to a table using a clamp, and instructed to move to its maximum displacement. The push-pull gauge was firmly attached to the tip of the controller, in opposition to the direction of motion.

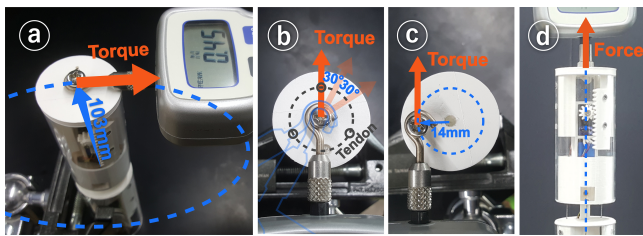


Figure 7: Setup for bending torque measurements in three different directions (a, b), for twisting torque (c), and stretching force (d).

To measure the bending and twisting torque we had first to determine the moment arm, as shown with blue arrows in Figure 7.a-c. Then we measured the force (i.e., orange arrows) to compute the torque values. Measurements were repeated 10 times, and, for the bending motion, we also considered three directions 30° apart (for a total of 30 samples in the range $0^\circ - 60^\circ$). The results showed that the GamesBond device can provide 34.78 N (SD: 0.88 N) of force when stretching/shrinking, and 13.51 N-cm (SD: 0.67 N-cm) of torque when twisting. Bending resulted in a wide range of torque measurements between a minimum of 25.86 N-cm (SD: 2.17 N-cm)

and a maximum of 37.49 N-cm (SD: 1.80 N-cm), depending on the direction of motion. This variation is rooted in the physical design of the tendons' actuation mechanism.

Finally, we conducted a pilot experiment with four participants (all males, aged between 22-27, M: 25.25 , SD: 2.22) in order to see whether typical grip forces would impede the controller's motions (i.e., grip force would result in stalling the motors). Because we could not directly measure in real-time the force applied by the motors, nor the deformations of the controller held in the hands, we used instead current as a proxy. The main purpose of this experiment is to verify whether the GamesBond devices properly reach the target position for a correct user's experience, even if the devices do not provide closed-loop control of force or position. Since the current is a good indicator that shows whether the motors meet the force limitation, we decided to indirectly check how often and how long the devices stall by reaching the maximum current threshold. We therefore equipped each of the internal five servomotors with a current sensor (ACS723) on the VCC rails, and sampled measurements of current at 210 Hz while users were asked to freely move the controllers for each of the three types of bond (rigid, soft, dynamic), each for one minute. For reference, we measured an average stall current of 653.6 mA (SD: 40.4) per servomotor. Using the measured data, we calculated the average current that each motor consumed and the percentage of time that motors were stalled. Figure 8 is the sample graph for one user, showing the current over time for each motor and the stall current threshold. Bending required on average

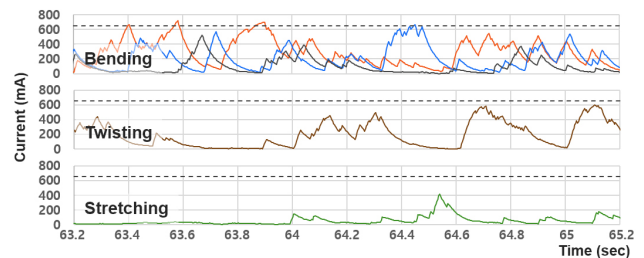


Figure 8: Current samples for three deformations of one participant over time. Dotted line indicates the stall current threshold.

207.9 mA, and resulted in stall for 4.57% of the total interaction time. Twisting and stretching required an average of 172.0 mA and 120.0 mA, resulting in stall respectively for 1.12% and 0.02% of the usage time.

4.3 Technical Evaluation Summary

In summary, through these technical evaluations we are able to determine that position control was accurate within 1.9° and 0.08 mm in any of direction of movement. It took at most 292.5 ms to configure the shape of the controllers within the maximum allowed ranges, exerting a mean torque of 13.51 N-cm for twisting, 25.86 N-cm for bending, and a mean force of 34.78 N for stretching. Finally, in the worst-case scenario, stall occurred 4.57% of the time, suggesting that a closed-loop feedback is not essential to for successful operation of the controllers during normal usage.

5 USER EVALUATION

Similarly to previous related work [16, 21], we conducted a user study to evaluate the perceived level of realism, immersion, and enjoyment of GamesBond for bimanual haptic feedback in VR. The study followed a within-subjects design with two factors – the *type of bond* between the controllers, and the *modality of feedback*. Specifically, each participant experienced three types of bonds (rigid, soft, dynamic) in two modality blocks (visual vs. haptic+visual). Conditions within the blocks were fully balanced, and the block order presentation was counterbalanced. The visual-only condition served as a baseline. In visual-only state the devices were turned on but steadily kept in zero-deformation state to perform as solid controller.

We recruited 12 participants (4 females, 8 males) aged 22-39 (M: 26.9, SD: 4.3) from the body of students in our institution. Eight participants previously experienced haptic devices, nine reported familiarity with VR, and seven with both haptics and VR.

After completing a demographics form, the participants wore the VIVE Pro HMD and held in their hand the GamesBond controllers. After a brief warm-up where the controllers operated as completely independent, users were requested to freely experience three types of bonds for at least one minute each. These were: a rigid bar, a soft deformable joint, and a dynamic rope capable of fluid motion, as described in the implementation section. Each type of bond was visually rendered using rigid and deformable bodies in Unity, as seen in Figure 5, but only in the haptic condition the controllers were actuated to provide haptic feedback. After experiencing each type of bond, the user rated on a 7-points Likert scale the perceived level of realism, immersion, and enjoyment of using the specified configuration. Finally, after experiencing all conditions and before concluding the experiment, we conducted a post-hoc interview to gather qualitative insights about the users' experiences. The experiment in total lasted about 20 minutes and participants were compensated 5 USD in local currency.

5.1 Results

Figure 9 shows an overview of the users ratings across conditions. Not surprisingly, the scores for all conditions augmented with haptics were significantly higher than those in the visual-only modality.

Specifically, a Wilcoxon signed rank test reveals statistically significant differences across all conditions ($p \leq 0.01$) for all the measured variables, with realism significant for rigid ($Z = -2.97$), soft ($Z = -2.82$) and dynamic ($Z = -2.81$) bonds. Similarly, immersion and enjoyment presented significant differences ($p \leq 0.01$) for rigid ($Z = -2.95$ and $Z = -2.96$) soft ($Z = -2.82$ and $Z = -2.96$) and dynamic ($Z = -2.72$ and $Z = -2.83$) bonds. We further analyzed the data to look for differences across bond type, performing a Friedman test followed by a Wilcoxon signed rank post-hoc test with Bonferroni corrections. Friedman test revealed a significant difference across bond types for realism ($\chi^2(2) = 12.4, p = 0.002$), immersion ($\chi^2(2) = 9.8, p = 0.007$), and enjoyment ($\chi^2(2) = 13.5, p = 0.001$). Post-hoc tests indicated that users perceived the rigid and soft connection different for all three measured variables ($p = 0.026$ for realism, $p = 0.044$ for immersion, and $p = 0.026$ for enjoyment) and between the rigid and dynamic bond for the enjoyment variable alone ($p = 0.016$).

The concluding interviews were proceeded in local language and analyzed using open and axial coding methods. All participants witnessed that the haptic feedback greatly enhanced the VR experience. Participants commented that "it was so realistic (P7)", "it felt like I'm swinging the real rope (P6)", and that "it's better than the Nintendo Wii (P7)". In comparison, users commented that the visual-only condition was "silly (P1, P11)" and "boring (P4)" because of the lack of haptic feedback.

Participants mostly appreciated the ability of feeling different characteristics for different connections ("It was great to experience feeling of different bars using one [pair of] devices" - P10), and the illusion of force/stiffness ("it felt that there was a force applied to the hands" - P11, or like "a physical exercise" - P5). When asked to comment whether the different bonds were clearly perceived, P12 commented that "it was surprising that haptic feedback felt differently depending on the type of connection". Most of the participants were therefore satisfied with the force exerted by the device, but some participants mentioned there was an adverse effect, as "the motor's power was so strong that I felt pulled by the motor (P12)"

We also gathered the participants' impressions on each separate bond and asked them to explain what mainly affected their ratings. Some participants explained that the reason why they felt the rigid bond less realistic than the soft or dynamic bonds was the absence of a noticeable visual effect, by saying "Because there was no visual deformation at all (P6)". Other participants picked the limited range of twisting and stretching as the main limitation of the rigid bond. P11 said "Stretching was so abrupt (because of the limited range of stretching of the device)", and P5 commented that "Twisting and stretching were so limited compared to bending".

Other participants also pointed out the limitations of the device. The most common comment was about the device's grip structure. P8, P9, and P12 mentioned the gap between the top and bottom segments of the device was disappointing and suggested including the two in a continuous enclosure. Several users also mentioned a mismatch between the shape of the physical controllers and the visual representation of the bonds. This resulted in accidentally bumping the controllers when moving them (P8, P9).

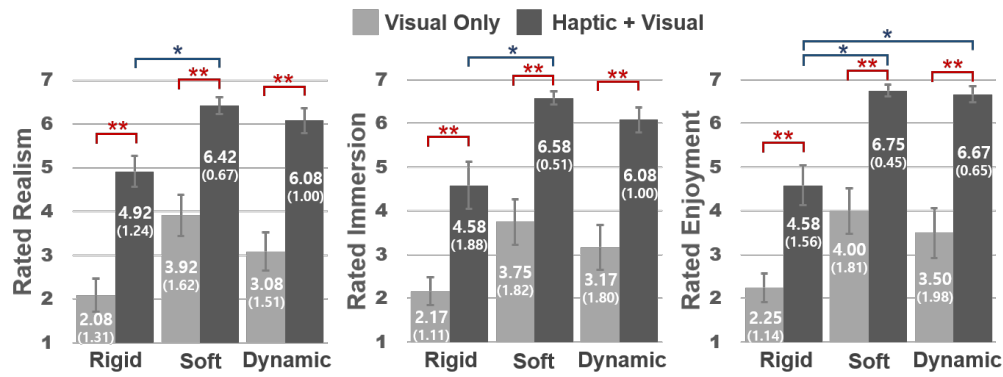


Figure 9: User evaluation results: mean scores (and standard deviation) displayed on the bars. The error bars represent the standard error of each variable.

Lastly, we gathered suggestions for possible application from participants. Most participants recommended leveraging on GamesBond’s ability to render varying stiffness to build fitness applications such as a jumping rope (P2, P4, P9, P10), power twisters (P3, P4, P5, P8, P9), or for simulating the sensation of grasping a steering wheel (P8). Other recommendations focused on creating illusions of forces, such as rendering a moving weight between two hands (P4, P6), the illusion of breaking a bar by abruptly changing the amount of bending (P3, P5), and pulling or pushing forces delivered through tools such as a fishing rod (P4). Finally, P2 and P7 suggested that GamesBond could not only be used by a single user, but also between people. We exemplify several of these applications in the next section of the paper.

In summary, both quantitative and qualitative metrics support our hypothesis that GamesBond increases the realism, immersion, and enjoyment of a VR experience. It also shows that our device can best render soft and dynamic bodies (e.g., a jumping rope), indicating possible avenues of explorations for future applications.

6 APPLICATIONS

To further illustrate the design space of the GamesBond controllers, we developed six VR applications using Unity 3D, and loosely grouped them into three categories: rendering 1) a jumping rope, 2) the illusion of force, and 3) various grip shapes.

6.1 Jumping rope

The jumping rope application best demonstrates the GamesBond’s unique capability of rendering the haptic sensation of a highly dynamic and deformable object. As shown in Figure 10.a, the user can experience a training session in a VR gym. Similarly to the dynamic rope used in the study, we constructed a longer jumping rope using the Obi Rope’s physics engine. The deformations of the controllers are then inferred by the rope geometry and used to update the shape of the controller. With our system, the user can jump as quickly as 60 hops per minute. It is also possible to change in software the parameters describing the physical characteristics of the rope (e.g., length, weight, thickness), which are immediately reflected in the physics simulation and the haptic rendering.

This scenario also supports two users interaction (Figure 10.b), with each user holding one extreme of the rope. Swinging the rope at one extreme, causes proportional movements on the other side, as in the physical world. To our knowledge, no previous haptic controller was capable of rendering the haptic illusion of a real rope in either the single or multi-users case.

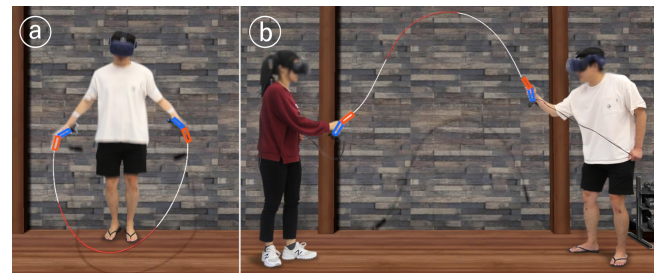


Figure 10: A jumping rope held by (a) one or (b) two people.

6.2 Force illusion

Previous work demonstrates that, given appropriate visual stimuli, skin deformations can trick a user in perceiving a force or load applied to the hands [8]. The GamesBond controllers leverage on the same effect, by using grip-deformations to instill the illusion of a force or load applied to the hands. In the *breaking-the-bar* application (Figure 11.a,b), users can attempt to bend a rigid wooden bar until it suddenly breaks. To render this effect, the controllers remain locked rigid until their position exceeded an angular threshold. At that point, the bending servos are released, resulting in an immediate (< 300 ms) transition from a stiff bond to no bond at all (i.e., the controllers are independent).

Another example of force illusion is the fishing application. The user can catch a fish using a fishing rod or a net held in two hands. A fish caught in the net would cause the controllers to bend proportionally to simulate its weight and relative location in the net (Figure 11.c). Similarly, a fishing rod would bend more or less depending on the location of the fish on the net. Differently from previous work which used a force-feedback applied to the wrist for

creating the illusion of a fishing rod [16], our approach allows for a similar effect without the need for large motors or fans (Figure 12).



Figure 11: Example applications that provides force illusion: *breaking-the-bar* (a, b) and *fishing net* (c).

6.3 Various grip shapes

The last group of applications shows how GamesBond controllers can be configured to render various object shapes and tools. Similarly to previous work which simulated different handles using the kinesthetic feedback of the physical linkage between the controllers [34], GamesBond controllers deform to mirror the shape of several construction tools based on the hands relative position (Figure 13). Furthermore, the absence of a physical constraining mechanism allows to rapidly switch between types of tools without mechanical delay or input sequences — for example, two independent electric screwdrivers can turn into a jackhammer in less than a second.

Perhaps more interestingly, the controllers can also be mapped to parts of an object with different functionalities, each with its own kinesthetic reference frame [1]. For example, the fishing rod described before, deforms one controller to simulate the bending of the pole, while the other simulates the motion of a winch. The user can spin the winch around an invisible axis orthogonal to the fishing pole, while the controller deforms to create this rotational effect. In this configuration each controller acts independently and conveys to the user different properties - the weight and position of the fish, and the tension caused by the winch.



Figure 12: In the *fishing rod* application, each controller expresses different features of the rod. The left controller renders bending of the rod, while the right simulates the motion of a winch.

7 LIMITATIONS AND CONCLUSION

We see numerous areas of possible improvements to GamesBond. The main limitations are related to the structural and mechanical



Figure 13: GamesBond applications rendering different grip shapes: a pair of separate electric screwdrivers with independent handles (a); a hammer drill with parallel handles (b); and a jackhammer with aligned handles (c).

design of the controllers. Using two separate and movable segments to render in-hand deformations is a simple solution that comes with several trade-offs. The min-max ranges of motions are limited, and in the case of bending, the torque is uneven depending on the direction of motion due to the placement of the internal tendons. The servo-motors are small in order to fit the controller’s body, but also slow and can only exert a limited force. In practice, oscillations faster than 1Hz cannot be realistically rendered [16], and a tight user grip could make ineffective the position control algorithm. This could be solved by, for example, using stronger and faster motors, placed outside the devices’ grip. Furthermore, we expect that closed-loop feedback and a faster refresh rate for the software calculation (currently 200Hz on average) could also mitigate the position control problem. Finally, the gap between the two segments of the controller can occasionally pinch the user’s skin, creating an unpleasant and unrealistic sensation. Although this rare situation only happened in the pilot study and was never observed in user evaluation, participants shared that this could be a concern to address in future iterations of the prototype. Future work will explore various shapes and sizes of the controllers, as well as exploring the effect of different gripping materials and textures applied to the handles. Theoretically, the controllers could also include multiple bending points for a more precise shape-changing mechanism.

The system evaluation presented in this paper also has numerous limitations due to the participant pool size, the lack of a psychophysics study that correlates grip-deformations to perceived forces (e.g., as in [8]), and the lack of a direct comparison with a physical bond (i.e., ground-truth). This work shows that the proposed approach supports the illusion of realistic bonds between the two controllers, but it does not characterize how it stacks up compared to mechanical alternatives (e.g., Haptic Links [34]) or other methods haptic modalities (e.g. vibrotactile feedback). Sound masking was not used in the realism study, as in prior work [18, 35], but we acknowledge that future work should investigate the effect of sound on immersion and enjoyment. Future work should further characterize the performance of GamesBond compared to other devices and explore experiences that go beyond gaming or simulations. For instance, the controllers could also be used for telepresence, teleoperation, and robotic manipulators [2, 17, 19].

Finally, we see an opportunity to enhance this work by adding sensing and input capabilities to the controllers. For example, by adding pressure or capacitive sensors as in [13], the system could

infer how tight is the user's grip, providing real-time feedback or adapting its behavior. The controllers could also include buttons, accelerometer, gyroscope, and magnetometer which would allow sensing micro-movements that might be difficult to pick up using the VIVE tracker. Using a sensor-fusion approach, the controllers could enable applications beyond gaming that require precise position tracking.

In conclusion, in this paper we introduced GamesBond, a pair of 4-DoF shape-changing controllers capable of creating the illusion of a virtual link connecting two controllers. We presented the overall mechanisms and described how rigid, soft, and dynamic connections can be simulated. The paper then introduces the details of the implementation, a technical evaluation of the position accuracy and force requirements necessary to correctly generate the grip deformations. A user study with 12 participants corroborates that our system improved the realism, immersion, and enjoyment of a VR experience. Finally, we presented a set of applications demonstrating practical usages of the systems, including force illusion, different grip shapes, and the first example of a virtual jumping rope.

ACKNOWLEDGMENTS

This work was supported by the National Research Foundation of Korea (NRF) grant funded by the Korea government (MSIT) (No. 2020R1A2C1012233).

REFERENCES

- [1] Ravin Balakrishnan and Ken Hinckley. 1999. The Role of Kinesthetic Reference Frames in Two-Handed Input Performance. In *Proceedings of the 12th Annual ACM Symposium on User Interface Software and Technology* (Asheville, North Carolina, USA) (UIST '99). Association for Computing Machinery, New York, NY, USA, 171–178. <https://doi.org/10.1145/320719.322599>
- [2] J. J. O. Barros, V. M. F. d. Santos, and F. M. T. P. d. Silva. 2015. Bimanual Haptics for Humanoid Robot Teleoperation Using ROS and V-REP. In *2015 IEEE International Conference on Autonomous Robot Systems and Competitions*. 174–179. <https://doi.org/10.1109/ICARSC.2015.27>
- [3] Sonny Chan, François Conti, Kenneth Salisbury, and Nikolas H Blevins. 2013. Virtual reality simulation in neurosurgery: technologies and evolution. *Neurosurgery* 72, suppl_1 (2013), A154–A164. <https://doi.org/10.1227/NEU.0b013e3182750d26>
- [4] Daniel KY Chen, Jean-Baptiste Chossat, and Peter B Shull. 2019. Haptivec: Presenting haptic feedback vectors in handheld controllers using embedded tactile pin arrays. In *Proceedings of the 2019 CHI Conference on Human Factors in Computing Systems*. 1–11. <https://doi.org/10.1145/3290605.3300401>
- [5] Eric J. Gonzalez and Sean Follmer. 2019. Investigating the Detection of Bimanual Haptic Retargeting in Virtual Reality. In *25th ACM Symposium on Virtual Reality Software and Technology* (Parramatta, NSW, Australia) (VRST '19). Association for Computing Machinery, New York, NY, USA, Article 12, 5 pages. <https://doi.org/10.1145/3359996.3364248>
- [6] Mar Gonzalez Franco and Christopher C Berger. 2019. Avatar Embodiment Enhances Haptic Confidence on the Out-of-Body Touch Illusion. *IEEE Transactions on Haptics* 12, 3 (June 2019), 319–326. <https://doi.org/10.1109/TOH.2019.2925038>
- [7] Yves Guiard. 1987. Asymmetric division of labor in human skilled bimanual action: The kinematic chain as a model. *Journal of motor behavior* 19, 4 (1987), 486–517. <https://doi.org/10.1080/00222895.1987.10735426>
- [8] Ashley L Guinan, Markus N Montandon, Andrew J Doxon, and William R Provancher. 2014. Discrimination thresholds for communicating rotational inertia and torque using differential skin stretch feedback in virtual environments. In *2014 IEEE Haptics Symposium (HAPTICS)*. IEEE, 277–282. <https://doi.org/10.1109/HAPTICS.2014.6775467>
- [9] Ashley L Guinan, Markus N Montandon, Andrew J Doxon, and William R Provancher. 2014. An ungrounded tactile feedback device to portray force and torque-like interactions in virtual environments. In *2014 IEEE Virtual Reality (VR)*. IEEE, 171–172. <https://doi.org/10.1109/VR.2014.6802106>
- [10] Takuya Handa, Makiko Azuma, Toshihiro Shimizu, and Satoru Kondo. 2017. GraspForm: Shape and Hardness Rendering on Handheld Device toward Universal Interface for 3D Haptic TV. In *Adjunct Publication of the 30th Annual ACM Symposium on User Interface Software and Technology*. 147–149. <https://doi.org/10.1145/3131785.3131824>
- [11] Tomás Henriques. 2019. SPRING Controller: An Interface for Kinesthetic Spatial Manipulation. In *2019 IEEE 7th International Conference on Serious Games and Applications for Health (SeGAH)*. IEEE, 1–5. <https://doi.org/10.1109/SeGAH.2019.8882478>
- [12] Seongkook Heo, Jaeyeon Lee, and Daniel Wigdor. 2019. PseudoBend: Producing haptic illusions of stretching, bending, and twisting using grain vibrations. In *Proceedings of the 32nd Annual ACM Symposium on User Interface Software and Technology*. 803–813. <https://doi.org/10.1145/3332165.3347941>
- [13] Ken Hinckley, Michel Pahud, Hrvoje Benko, Pourang Irani, François Guimbretière, Marcel Gavrilu, Xiang 'Anthony' Chen, Fabrice Matulic, William Buxton, and Andrew Wilson. 2014. Sensing Techniques for Tablet+stylus Interaction. In *Proceedings of the 27th Annual ACM Symposium on User Interface Software and Technology* (Honolulu, Hawaii, USA) (UIST '14). Association for Computing Machinery, New York, NY, USA, 605–614. <https://doi.org/10.1145/2642918.2647379>
- [14] Ken Hinckley, Koji Yatani, Michel Pahud, Nicole Coddington, Jenny Rodenhuse, Andy Wilson, Hrvoje Benko, and Bill Buxton. 2010. Pen + Touch = New Tools. In *Proceedings of the 23rd Annual ACM Symposium on User Interface Software and Technology* (New York, New York, USA) (UIST '10). Association for Computing Machinery, New York, NY, USA, 27–36. <https://doi.org/10.1145/1866029.1866036>
- [15] Yuki Imamura, Hironori Arakawa, Sho Kamuro, Kouta Minamizawa, and Susumu Tachi. 2011. HAPMAP: Haptic walking navigation system with support by the sense of handrail. In *ACM SIGGRAPH 2011 Emerging Technologies*. 1–1. <https://doi.org/10.1145/2048259.2048265>
- [16] Seungwoo Je, Myung Jin Kim, Woojin Lee, Byungjoo Lee, Xing-Dong Yang, Pedro Lopes, and Andrea Bianchi. 2019. Aero-plane: A Handheld Force-Feedback Device that Renders Weight Motion Illusion on a Virtual 2D Plane. In *Proceedings of the 32nd Annual ACM Symposium on User Interface Software and Technology*. 763–775. <https://doi.org/10.1145/3332165.3347926>
- [17] Oussama Khatib, Xiyang Yeh, Gerald Brantner, Brian Soe, Boyeon Kim, Shameek Ganguly, Hannah Stuart, Shiquan Wang, Mark Cutkosky, Aaron Edsinger, et al. 2016. Ocean one: A robotic avatar for oceanic discovery. *IEEE Robotics & Automation Magazine* 23, 4 (2016), 20–29. <https://doi.org/10.1109/MRA.2016.2613281>
- [18] Andrey Krehhov, Katharina Emmerich, Philipp Bergmann, Sebastian Cmentowski, and Jens Krüger. 2017. Self-transforming controllers for virtual reality first person shooters. In *Proceedings of the Annual Symposium on Computer-Human Interaction in Play*. 517–529. <https://doi.org/10.1145/3116595.3116615>
- [19] Alexander Kron, Günther Schmidt, Bernd Petzold, Michael I Zah, Peter Hinterseer, and Eckehard Steinbach. 2004. Disposal of explosive ordnances by use of a bimanual haptic telepresence system. In *IEEE International Conference on Robotics and Automation, 2004. Proceedings. ICRA'04. 2004, Vol. 2*. IEEE, 1968–1973. <https://doi.org/10.1109/ROBOT.2004.1308112>
- [20] Michael A Liss and Elspeth M McDougall. 2013. Robotic surgical simulation. *The Cancer Journal* 19, 2 (2013), 124–129. <https://doi.org/10.1097/PPO.0b013e3182885d79>
- [21] Pedro Lopes, Sijing You, Lung-Pan Cheng, Sebastian Marwecki, and Patrick Baudisch. 2017. Providing Haptics to Walls & Heavy Objects in Virtual Reality by Means of Electrical Muscle Stimulation. In *Proceedings of the 2017 CHI Conference on Human Factors in Computing Systems* (Denver, Colorado, USA) (CHI '17). Association for Computing Machinery, New York, NY, USA, 1471–1482. <https://doi.org/10.1145/3025453.3025600>
- [22] Benjamin C Mac Murray, Bryan N Peele, Patricia Xu, Josef Spjut, Omer Shapira, David Luebke, and Robert F Shepherd. 2018. A variable shape and variable stiffness controller for haptic virtual interactions. In *2018 IEEE International Conference on Soft Robotics (RoboSoft)*. IEEE, 264–269. <https://doi.org/10.1109/ROBOSOF.2018.8404930>
- [23] Miles Macklin, Matthias Müller, and Nuttapong Chentanez. 2016. XPBD: Position-Based Simulation of Compliant Constrained Dynamics. In *Proceedings of the 9th International Conference on Motion in Games* (Burlingame, California) (MIG '16). Association for Computing Machinery, New York, NY, USA, 49–54. <https://doi.org/10.1145/2994258.2994272>
- [24] Jun Murayama, Laroussi Bougrila, YanLin Luo, Katsuhito Akahane, Shoichi Hasegawa, Béat Hirsbrunner, and Makoto Sato. 2004. SPIDAR G&G: a two-handed haptic interface for bimanual VR interaction. In *Proceedings of EuroHaptics*, Vol. 2004. Citeseer, 138–146.
- [25] Ken Nakagaki, Chikara Inamura, Pasquale Totaro, Thariq Shihpar, Chantane Akikyama, Yin Shuang, and Hiroshi Ishii. 2015. Linked-Stick: Conveying a Physical Experience Using a Shape-Shifting Stick. In *Proceedings of the 33rd Annual ACM Conference Extended Abstracts on Human Factors in Computing Systems* (Seoul, Republic of Korea) (CHI EA '15). Association for Computing Machinery, New York, NY, USA, 1609–1614. <https://doi.org/10.1145/2702613.2732712>
- [26] MJ Patel, JHY Ng, WE Hawkins, KF Pitts, and S Chakrabarti-Bell. 2012. Effects of fungal α -amylase on chemically leavened wheat flour doughs. *Journal of cereal science* 56, 3 (2012), 644–651. <https://doi.org/10.1016/j.jcs.2012.08.002>
- [27] Angelika Peer and Martin Buss. 2008. A new admittance-type haptic interface for bimanual manipulations. *IEEE/ASME Transactions on mechatronics* 13, 4 (2008),

- 416–428. <https://doi.org/10.1109/TMECH.2008.2001690>
- [28] Ken Pfeuffer, Ken Hinckley, Michel Pahud, and Bill Buxton. 2017. Thumb + Pen Interaction on Tablets. In *Proceedings of the 2017 CHI Conference on Human Factors in Computing Systems* (Denver, Colorado, USA) (CHI '17). Association for Computing Machinery, New York, NY, USA, 3254–3266. <https://doi.org/10.1145/3025453.3025567>
- [29] Tomoya Sasaki, Richard Sahala Hartanto, Kao-Hua Liu, Keitarou Tsuchiya, Atsushi Hiyama, and Masahiko Inami. 2018. Leviopole: mid-air haptic interactions using multirotor. In *ACM SIGGRAPH 2018 Emerging Technologies*. 1–2. <https://doi.org/10.1145/3214907.3214913>
- [30] Jotaro Shigeyama, Takeru Hashimoto, Shigeo Yoshida, Takuji Narumi, Tomohiro Tanikawa, and Michitaka Hirose. 2019. Transcalibur: A weight shifting virtual reality controller for 2d shape rendering based on computational perception model. In *Proceedings of the 2019 CHI Conference on Human Factors in Computing Systems*. 1–11. <https://doi.org/10.1145/3290605.3300241>
- [31] Peng Song, Wooi Boon Goh, William Hutama, Chi-Wing Fu, and Xiaopei Liu. 2012. A Handle Bar Metaphor for Virtual Object Manipulation with Mid-Air Interaction. In *Proceedings of the SIGCHI Conference on Human Factors in Computing Systems* (Austin, Texas, USA) (CHI '12). Association for Computing Machinery, New York, NY, USA, 1297–1306. <https://doi.org/10.1145/2207676.2208585>
- [32] Adam J Spiers and Aaron M Dollar. 2016. Design and evaluation of shape-changing haptic interfaces for pedestrian navigation assistance. *IEEE transactions on haptics* 10, 1 (2016), 17–28. <https://doi.org/10.1109/TOH.2016.2582481>
- [33] Adam J Spiers, Janet van Der Linden, Maria Oshodi, and Aaron M Dollar. 2016. Development and experimental validation of a minimalistic shape-changing haptic navigation device. In *2016 IEEE International Conference on Robotics and Automation (ICRA)*. IEEE, 2688–2695. <https://doi.org/10.1109/ICRA.2016.7487430>
- [34] Evan Strasnick, Christian Holz, Eyal Ofek, Mike Sinclair, and Hrvoje Benko. 2018. Haptic links: Bimanual haptics for virtual reality using variable stiffness actuation. In *Proceedings of the 2018 CHI Conference on Human Factors in Computing Systems*. 1–12. <https://doi.org/10.1145/3173574.3174218>
- [35] Yuqian Sun, Shigeo Yoshida, Takuji Narumi, and Michitaka Hirose. 2019. Pacapa: A handheld vr device for rendering size, shape, and stiffness of virtual objects in tool-based interactions. In *Proceedings of the 2019 CHI Conference on Human Factors in Computing Systems*. 1–12. <https://doi.org/10.1145/3290605.3300682>
- [36] Colin Swindells, Alex Unden, and Tao Sang. 2003. TorqueBAR: an ungrounded haptic feedback device. In *Proceedings of the 5th international conference on Multimodal interfaces*. 52–59. <https://doi.org/10.1145/958432.958445>
- [37] Shan-Yuan Teng, Tzu-Sheng Kuo, Chi Wang, Chi-huan Chiang, Da-Yuan Huang, Liwei Chan, and Bing-Yu Chen. 2018. PuPoP: Pop-up Prop on Palm for Virtual Reality. In *Proceedings of the 31st Annual ACM Symposium on User Interface Software and Technology* (Berlin, Germany) (UIST '18). Association for Computing Machinery, New York, NY, USA, 5–17. <https://doi.org/10.1145/3242587.3242628>
- [38] Julie M Walker, Nabil Zemiti, Philippe Poinet, and Allison M Okamura. 2019. Holdable haptic device for 4-dof motion guidance. In *2019 IEEE World Haptics Conference (WHC)*. IEEE, 109–114. <https://doi.org/10.1109/WHC.2019.8816171>
- [39] Shigeo Yoshida, Yuqian Sun, and Hideaki Kuzuoka. 2020. PoCoPo: Handheld Pin-based Shape Display for Haptic Rendering in Virtual Reality. In *Proceedings of the 2020 CHI Conference on Human Factors in Computing Systems*. 1–13. <https://doi.org/10.1145/3313831.3376358>
- [40] Andre Zenner and Antonio Krüger. 2017. Shifty: A weight-shifting dynamic passive haptic proxy to enhance object perception in virtual reality. *IEEE transactions on visualization and computer graphics* 23, 4 (2017), 1285–1294. <https://doi.org/10.1109/TVCG.2017.2656978>
- [41] André Zenner and Antonio Krüger. 2019. Drag: on: A virtual reality controller providing haptic feedback based on drag and weight shift. In *Proceedings of the 2019 CHI Conference on Human Factors in Computing Systems*. 1–12. <https://doi.org/10.1145/3290605.3300441>